IEEE Access
Multidisciplinary | Rapid Review | Open Access Journal

Received August 28, 2020, accepted September 11, 2020, date of publication October 13, 2020, date of current version October 22, 2020.

Digital Object Identifier 10.1109/ACCESS.2020.3030637

Two-Stage Congestion Management Considering Virtual Power Plant With Cascade Hydro-Photovoltaic-Pumped Storage Hybrid Generation

NAN LOU[1], YONG ZHANG[1], YUQIN WANG[2], QIXING LIU[1], HUIYONG LI[1], YU SUN[2], AND ZONGTIAN GUO[2]

[1]China Southern Power Grid Company Ltd., Guangzhou 510663, China
[2]Dongfang Electronics Company Ltd., Yantai 264001, China

Corresponding author: Yu Sun (1437872483@qq.com)

ABSTRACT With the widespread access of flexible loads and renewable energy, the power flow often exceeds the limit of line, resulting in the blockage of distribution network. Virtual power plant (VPP) can not only integrate multiple forms of energy, but also improve the penetration proportion of renewable energy sources. In view of the excellent ability of VPP in power market, a two-stage congestion management (CM) model involving virtual power plant (VPP) with cascade hydro-photovoltaic-pumped storage hybrid generators is established in this paper. The first stage is congestion management of ISO (Independent System Operator), which aims at minimizing congestion cost and is solved by genetic algorithm. The second stage is power correction model of virtual power plant, which is a multi-objective problem considering water and light curtailment, navigation and ecological needs. An improved hybrid non-dominated sorting genetic algorithm-II (HNSGA-II) is proposed to solve the two-stage model. Case studies show that the participation of virtual power plants in congestion management has certain economic value to power system. The joint dispatch of cascade hydro-photovoltaic-pumped storage hybrid generation in the virtual power plant can make flexible decisions according to the needs of energy saving, navigation and ecology. The improved HNSGA-II algorithm is superior to the traditional NSGA-II algorithm in convergence, uniformity and extensity.

INDEX TERMS Cascade hydropower, congestion management, multi-objective optimization, virtual power plant.

NOMENCLATURE

VARIABLES

$Q^H_{i,t}/Z_{i,t}$	Power generation flow/water level of cascade hydropower station i at time t
$P^{hy}_{i,t}$	Active power output of cascade hydropower station i at time t
$H_{i,t}/V_{i,t}/S_{i,t}$	Net water head/capacity/discharge of cascade hydropower station i at time t
$P^{pv,\max}_{j,t}/P^{pv}_{j,t}$	Maximum/actual power output of photovoltaic power station j at time t
$P^{pg}_{k,t}/P^{pp}_{k,t}$	Generation/pumped active power of pumped storage units k at time t
$\Delta P^{Vpp,up}_t/\Delta P^{Vpp,down}_t$	Up/down generation adjustment of virtual power plant at time t after congestion management
$\Delta P^{G,up}_{p,t}/\Delta P^{G,down}_{p,t}$	Up/down generation adjustment of conventional unit p at time t after congestion management
$IL_{q,t}$	Load shedding of node q at time t after congestion management
F	Objective of ISO congestion management model

The associate editor coordinating the review of this manuscript and approving it for publication was Feng Wu.

P_t^m/Q_t^m	Avtive/reactive power output of node m at time t
V_t^m	Voltage of node m at time t
θ_t^{mn}	Phase angle difference of node m and n at time t
$Q_{p,t}^G$	Reactive power output of unit p at time t
$P_{p,t}^G/P_t^{Vpp}$	Active power output of conventional unit p/virtual power plant at time t
F_i	Objective i of VPP power correction model
$f_{i,t}^{Nav}$	Navigation satisfaction of cascade hydropower station i at time t
f_i^{Eco}	Ecology satisfaction of cascade hydropower station i at time t
x'/v_k'	solution/solution components after variation
x	Decision variables set of improved HNSGA-II algorithm
$f\ (x)$	Objective function vector of improved HNSGA-II algorithm
$g_j\ (x)$	Inequality constraint j of improved HNSGA-II algorithm
$h_j\ (x)$	Equality constraint j of improved HNSGA-II algorithm
$f_i'\ (x)$	The ith modified objective value of x
$d_i\ (x)$	Distance value of ith modified objective
$p_i\ (x)$	Penalty term of ith modified objective
α	Feasible solution ratio
$\bar{f}_i\ (x)$	Normalization value of ith modified objective
$f_i^{\min}$	Minimum value of ith modified objective
$f_i^{\max}$	Maximum value of ith modified objective
$C\ (x)$	Constraint deviation value of x
E	Real pareto front
n_E	Number of solutions in real pareto front
$n_{P^k \bigcap E}$	Number of solutions in set $P^k \bigcap E$
$d_{k,i}$	Distance of solution i of algorithm k
$\overline{d_k}$	Average distance of algorithm k
$C_k/S_k/MS_k$	convergence/uniformity/extensity of algorithm k
$f_k^{j,\max}/f_k^{j,\min}$	Maximum/minimum value of jth objective in kth algorithm's pareto front
$F^{j,\max}/F^{j,\min}$	Maximum/minimum value of jth objective in E

PARAMETERS

T	Dispatch period of VPP
Δt	Length of dispatch period T
$n_{hy}/n_{pv}/n_p$	Total number of cascade hydropower stations/photovoltaic power stations/pumped storage units
a_{1i}, b_{1i}, c_{1i}	Tail water lever coefficients of cascade hydropower station i
a_{2i}, c_{2i}	Head loss coefficient of cascade hydropower station i
$I_{i,t}$	Inflow of cascade hydropower station i at time t
$a_{3i}, b_{3i}, c_{3i}, d_{3i}$	Capacity to water level coefficient of cascade hydropower station i
$Z_{i,t}^{\min}/Z_{i,t}^{\max}$	Minimum/maximum water level of cascade hydropower station i at time t
$\overline{Z}_i/Z_{i,\mathrm{T}}$	Original/time T water level of cascade hydropower station i
$Q_{i,t}^{H\,\min}/Q_{i,t}^{H\,\max}$	Minimum/Maximum power generation flow of cascade hydropower station i at time t
$S_{i,t}^{\max}$	Maximum discharge of cascade hydropower station i at time t
$\eta_{hy}/\eta_{pv}/\eta_p$	Efficiency of cascade hydropower/photovoltaic power generation/pumped storage units
$\Delta Z_i^{\mathrm{D}\,\max}$	Upper limit of water level variation of cascade hydropower station i
$\Delta Z_i^{\mathrm{H}\,\max}$	Water level climbing limit of cascade hydropower station i
$S_i^{\mathrm{E}\,\min}$	Minimum ecological flow of cascade hydropower station i
A_s	Rated irradiance of photovoltaic power station
$T_{j,t}^{STC}$	Actual temperature of photovoltaic power station j at time t
$A_{j,t}$	Actual irradiance of photovoltaic power station j at time t
α_p	Temperature power coefficient
T^{pv}	Temperature of photovoltaic modules under standard test conditions
$P_{rate,j}^{pv}$	Rated power of photovoltaic power station j
$P_{rate,k}^{p}$	Rated power of pumped storage unit k
$c_p^{G,up}/c_p^{G,down}$	Up/down generation adjustment cost of pth conventional unit participating in congestion management
$c^{Vpp,up}/c^{Vpp,down}$	Up/down generation adjustment cost of pth VPP participating in congestion management
$VOLL$	Load shedding cost of congestion management
n_G/n_D	Number of conventional units/reducible loads participating in congestion management
$P_{m,t}^D$	Load of node m at time t
$P_{p,t}^{G,0}/P_t^{Vpp,0}$	Power of pth conventional unit/VPP

	at time t before congestion management
M	Number of nodes
$G_{mn}/B_{mn}/P_{\max}^{L,mn}$	Conductance/susceptance/power limits of line mn
$V_{\min}^{m}/V_{\max}^{m}$	Lower/upper voltage limits of node m
$P_{t_1,t_2}^{load,m}/Q_{t_1,t_2}^{load,m}$	Active/reactive loads of node m at month $t_1$period t_2
$P_{\min}^{G}/P_{\max}^{G}$	Power output limits of conventional units in main grid
$S_i^{Eco}/S_i^{E\min}$	Ideal/minimum ecological needed flow of cascade hydropower station i
it	Current iteration of evolution algorithm
$Imax$	Maximum number of iterations
β	Coefficient of non-uniform variation, usually between 2 and 5
r	Random number between 0 and 1
rnd	0 or 1
δ	Local search coefficient
q	Number of inequality constraints of VPP power correction model
p	Number of constraints of VPP power correction model
ε	Relaxation of improved HNSGA-II algorithm
P^k	Pareto front of kth algorithm
$f_{k,i}^{j}$	jth objective for ith solution of kth algorithm
n	Number of objective
$F_{\min}^{Eco}$	Minimum ecological satisfaction index

I. INTRODUCTION

With the over-exploitation of fossil energy and the worsening of the ecological environment, environmental issues have become more and more important. Countries around the world are actively promoting the development of renewable energy sources to control greenhouse gases. As a mature technology, hydropower is an important way to achieve green power. Regarding the optimal dispatching strategy of hydropower, authors in [1] introduced the Gini coefficient to reflect the equilibrium degree of cascade hydropower distribution, and established an optimization model for cascade reservoirs considering the degree of equilibrium and peak regulation tasks before the flood. Authors in [2] proposed a short-term scheduling strategy of pumping and storage units, and transformed it into a linear model for solving. Many scholars have also studied the needs for navigation and ecology while considering the power generation characteristics of hydropower units. In [3], a multi-objective optimization model for hydropower generation, ecology and navigation was established. Authors in [4] built a multi-objective model of peak shaving and shipping, and used the principles of proximity and marginal analysis to balance the model's peak shaving demand and navigation demand.

Photovoltaic is also a fast-developing renewable energy, which is intermittent and fluctuating. It requires other energy sources to provide backup support, and it is usually integrated with other types of power sources for scheduling. Authors in [5] established a probabilistic model, and processed the correlation of photovoltaic power generation through Nataf transformation. Authors in [6] and [7] established a coordinated scheduling model for photovoltaic, hydropower and carbon capture power plants, and proposed an active water abandonment strategy to improve water resource utilization. Authors in [8] analyzed the coordination ability of multiple sources of energy in the high and low water season models to increase the on-line utilization rate of scenery through nuclear power and hydropower.

In an open electricity market, power plants supply power to consumers through transmission lines. Blockage occurs when the line capacity cannot meet market demand. The main method for congestion management (CM) is through rescheduling of generating units, and this method in [9] is low cost and simple. On the other hand, with the large-scale influx of distributed power sources and energy storage devices, more and more nodes in the distribution network have greater initiative, and many scholars have begun to study the issue of power system congestion management with load participation. Authors in [10] used nodal electricity price to establish a multi-period demand response model for congestion management. Authors in [11] proposed an input-output-based interruption loss evaluation method for modeling interruptible loads, and established a congestion management model for coordinating unit output and interruptible load for DC power flow. Authors in [12] analyzed the problem of transmission congestion in the inter-regional interconnected power market, integrating demand response resources such as demand elasticity, temperature-controlled loads, and interruptible loads. Authors in [13] and [14] established an incentive-based demand response model and studied its scheduling strategy for participating in congestion management. In [15], the congestion management model was divided into two stages and solved by Benders decomposition.

The congestion management models in the above articles are all single-objective models and aim at minimizing the cost of congestion. Many literatures have turned congestion management problems into multi-objective optimization models. The goals of blocking management in [16] include minimum blocking cost, voltage stability and dynamic stability. A hybrid algorithm combining improved ε-constraint method and weighted method is proposed. A voltage-dependent load model was established in [17], and the congestion management objectives included maximizing the load and demand response, etc., which is solved by an improved multi-objective enhanced Pareto evolutionary algorithm. Authors

in [18] proposed a multi-objective algorithm based on standard orthogonal constraints that can obtain a uniform and effective Pareto front to solve the blocking management objectives, which included blocking cost, voltage stability and transient stability. However, the demand side resources involved in congestion management are relatively simple in the existing literature. This paper considers virtual power plants (VPP) that integrate multiple resources in congestion management. Then, the congestion management problem becomes a two-stage optimization problem including an ISO congestion management model and a VPP power correction model, which is a multi-objective nonlinear problem.

Due to the outstanding performance of local search ability and global convergence, NSGA-II is widely used to get the Pareto solutions for multi-ojective problems. In [19], HNSGA-II was proposed based on NSGA-II. The improvement of HNSGA-II is to add non-uniform operator and local search progress to each NSGA-II iteration to improve the extensity and accuracy of non-dominated solutions of each iteration. In this paper, we improve HNSGA-II to obtain better Pareto fronts.

The main contributions of this paper are:

1. This paper established an optimization model of virtual power plant with cascade hydro-photovoltaic-pumped storage hybrid generators to integrate multiple energy resources.
2. This paper built a two-stage congestion management model, including an ISO congestion management model and a virtual power plant power correction model.
3. This paper proposed an improved HNSGA-II algorithm to solve the multi-objective optimization problems, which improved the diversity and convergence of the solution.

II. OPTIMIZATION MODEL OF VIRTUAL POWER PLANT

A. CASCADE HYDROPOWER UNITS

Hydropower stations are not only used to meet the power generation needs of the power system, but also undertake many tasks such as water use and shipping. For cascaded hydropower systems, this paper models from three aspects: power generation, navigation, and ecology.

1) GENERATION CONSTRAINTS

$$P_{i,t}^{hy} = \eta_{hy} Q_{i,t}^{H} H_{i,t} \Delta t \tag{1}$$

$$H_{i,t} = 0.5\left(Z_{i,t-1} + Z_{i,t}\right) - \left(a_{1i} S_{i,t}^{2} + b_{1i} S_{i,t} + c_{1i}\right) - \left(a_{2i}\left(Q_{i,t}^{H}\right)^{2} + c_{2i}\right) \tag{2}$$

$$V_{i,t+1} = V_{i,t} + 3600\left(I_{i,t} + S_{i-1,t} - S_{i,t}\right)\Delta t \tag{3}$$

$$Z_{i,t} = a_{3i}\left(V_{i,t}\right)^{3} + b_{3i}\left(V_{i,t}\right)^{2} + c_{3i} V_{i,t} + d_{3i} \tag{4}$$

$$Z_{i,\mathrm{T}} = \overline{Z}_i \tag{5}$$

$$Z_{i,t}^{\min} \le Z_{i,t} \le Z_{i,t}^{\max} \tag{6}$$

$$Q_{i,t}^{H\,\min} \le Q_{i,t}^{H} \le Q_{i,t}^{H\,\max} \tag{7}$$

$$S_{i,t} \le S_{i,t}^{\max} \tag{8}$$

$$Q_{i,t}^{H} \le S_{i,t} \tag{9}$$

$$P_{i,t}^{hy} \le P_{rate,i}^{hy} \tag{10}$$

Equation (1) represents the power generation of cascade hydropower. Equation (2) represents the net water head, and the first term on the right side of the equation represents the water level in the front pond, the second term is the tail water level, and the third term represents the head loss. Equation (3)-(10) represent the relationship between the storage capacity and the discharge flow, the relationship between the storage capacity and the storage water level, termination of the storage water level constraint, the storage water level upper and lower limit constraints, the head upper and lower limit constraints, the discharge flow upper limit constraint, the water curtailment constraint, and the power limit constraint.

2) NAVIGATION CONSTRAINTS

$$\max\left(Z_{i,t}\right) - \min\left(Z_{i,t}\right) \le \Delta Z_i^{\mathrm{D}\max} \tag{11}$$

$$\max\left(\mathrm{abs}\left(Z_{i,t} - Z_{i,t-1}\right)\right) \le \Delta Z_i^{\mathrm{H}\max} \tag{12}$$

Equation (11) represents the daily water level variation limit. Equation (12) represents the water level climbing restriction.

3) ECOLOGICAL CONSTRAINTS

$$\sum_{t}^{T} S_{i,t} \ge S_i^{\mathrm{E}\min} \tag{13}$$

$$f_i^{Eco} = \begin{cases} 1 & \sum_{t}^{T} S_{i,t}^{H} > S_i^{Eco} \\ \dfrac{\sum_{t}^{T} S_{i,t}^{H}}{S_i^{Eco}} & \sum_{t}^{T} S_{i,t}^{H} \le S_i^{Eco} \end{cases} \tag{14}$$

$$F^{Eco} = \sum_{i}^{n_{hy}} f_i^{Eco} \ge F_{\min}^{Eco} \tag{15}$$

In this paper, the power dispatching period and the navigation requirements of cascade hydropower are considered in hours. The period of ecological constraints and objectives is in days. Equation (13) indicates that the reservoir discharge must meet certain ecological requirements within a day. Equation (14) represents the calculation of the ecological satisfaction index. Equation (15) indicates that the cascade hydropower has to meet certain ecological satisfaction index constraints.

B. PHOTOVOLTAIC POWER GENERATION MODEL

The output of photovoltaic unit is related to factors such as irradiance and temperature. The power equation can be expressed as (16), and (17) indicates that the actual

photovoltaic output is less than the allowed maximum output.

$$P_{j,t}^{pv,\max} = \eta_{pv} P_{rate,j}^{pv} \frac{A_{j,t}}{A_s} \left[1 + \alpha_p \left(T^{pv} - T_{j,t}^{STC}\right)\right] \quad (16)$$

$$0 \le P_{j,t}^{pv} \le P_{j,t}^{pv,\max} \quad (17)$$

C. PUMPED STORAGE POWER GENERATION MODEL

Pumped-storage power stations can stabilize network power fluctuations, and are divided into two states: pumping and power generation. The model is shown below.

$$P_{k,t}^{pg} P_{k,t}^{pp} = 0 \quad (18)$$

$$\sum_{t}^{T} P_{k,t}^{pg} - \eta_p \sum_{t}^{T} P_{k,t}^{pp} = 0 \quad (19)$$

$$0 \le P_{k,t}^{pg}, P_{k,t}^{pp} \le P_{rate,k}^{p} \quad (20)$$

Equation (18) indicates that the pumped storage unit can only be one state (pumping or power generation). Equation (19) indicates the power balance constraint of the pumped storage unit in a dispatch period, and (20) indicates the upper and lower limit constraints of power generation and pumping.

III. CONGESTION MANAGEMENT MODEL

A. MARKET FRAMEWORK OF CONGESTION MANAGEMENT

The bilateral deregulated electricity market allows the participation of demand side resources, and virtual power plants as independent economic entities can participate in congestion management. The market operation mechanism is shown in Figure 1. The market players include power producers, virtual power plants, and interruptible loads. When power system congestion occurs, the virtual power plant and power generator formulate a congestion adjustment strategy, and submit the offer and the maximum power generation adjustment amount to ISO. The ISO clears the market with the goal of minimizing the cost of congestion management, and then sends back the results to various market participants. The virtual power plant optimizes dispatching of cascade hydropower, photovoltaic, and pumped storage according to the market clearance results, and updates its response strategy. In this paper, a two-stage optimization model for congestion management with a virtual power plant is established. The first stage is an ISO congestion management model, and the second stage is a virtual power plant power correction model, as shown in the next section.

B. ISO CONGESTION MANAGEMENT MODEL

In order to ensure the economical and safe operation of the power system, ISO is responsible for checking whether the power system is congested. When the system is congested, ISO takes the minimum cost of congestion as the objective and reschedules the power generation side and demand side.

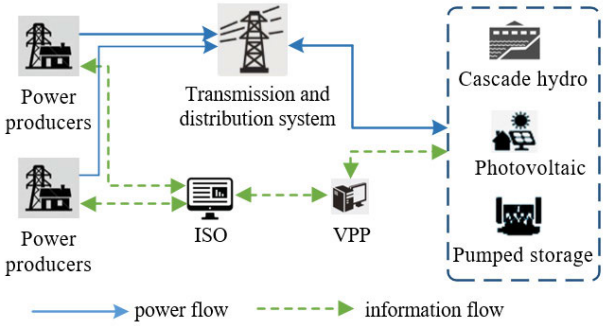

FIGURE 1. The CM market framework of power system with VPPs.

The congestion management model can be expressed as:

$$\min F = \sum_{t}^{T} \left\{ \sum_{p}^{n_G} \left(c_p^{G,up} \Delta P_{p,t}^{G,up} + c_p^{G,down} \Delta P_{p,t}^{G,down} \right) + \left(c^{Vpp,up} \Delta P_t^{Vpp,up} + c^{Vpp,down} \Delta P_t^{Vpp,down} \right) + VOLL \sum_{q}^{n_D} IL_{q,t} \right\} \quad (21)$$

$$P_t^m = V_t^m \sum_{n}^{M} V_t^n \left(G_{mn} \cos\theta_t^{mn} + B_{mn} \sin\theta_t^{mn} \right) \quad (22)$$

$$Q_t^m = V_t^m \sum_{n}^{M} V_t^n \left(G_{mn} \sin\theta_t^{mn} - B_{mn} \cos\theta_t^{mn} \right) \quad (23)$$

$$P_t^m = \sum_{p \in m}^{P_{p,t}^G} + P_t^{Vpp} + IL_{m,t} - P_{m,t}^D \quad Vpp \in m \quad (24)$$

$$Q_t^m = \sum_{p \in m}^{Q_{p,t}^G} \quad (25)$$

$$P_{p,t}^G = P_{p,t}^{G,0} + \Delta P_{p,t}^{G,up} - \Delta P_{p,t}^{G,down} \quad (26)$$

$$P_t^{Vpp} = P_t^{Vpp,0} + \Delta P_t^{Vpp,up} - \Delta P_t^{Vpp,down} \quad (27)$$

$$-P_{\max}^{L,mn} \le \left| V_t^m V_t^n \left(G_{mn} \cos\theta_t^{mn} - B_{mn} \sin\theta_t^{mn} \right) \right| \le P_{\max}^{L,mn} \quad (28)$$

$$V_{\min}^m \le V_t^m \le V_{\max}^m \quad (29)$$

$$P_{\min}^G \le P_{p,t}^G \le P_{\max}^G \quad (30)$$

$$\sum_{k} -P_{rate,k}^{P} \le P_t^{VPP} \le \sum_{k} P_{rate,k}^{P} + \sum_{j} P_{j,t}^{pv,\max} \quad (31)$$

In day-ahead market, the clearing prices of different nodes are the same when the network is uncongested. But if the network is congested, conventional units and VPP will offer power adjustment prices and adjust the corresponding outputs to eliminate congestion, which can be considered as a kind of ancillary service. Equation (21) indicates that the congestion management goal is to minimize congestion costs.

The first term represents the adjustment costs of the conventional units. The second term represents the power adjustment costs of VPP, and the third term represents load shedding costs. Equations (22) and (23) represent active and reactive power flow equations. Equations (24) and (25) represent active and reactive power injection into nodes respectively. Equations (26) and (27) represent the outputs of generators and VPP after congestion management. Equations (28)-(31) respectively represent the line power flow limit, node voltage limit, conventional unit output and VPP output limits.

C. VIRTUAL POWER PLANT POWER CORRECTION MODEL

After the ISO performs congestion management, the virtual power plant performs power adjustments based on the congestion adjustments issued by the ISO. In this paper, the operating costs of hydropower and photovoltaic units are not taken into consideration, and the objectives of the virtual power plant power correction model include the amount of water and light curtailment, as shown below.

1) WATER AND LIGHT CURTAILMENT TARGET

Equation (32) represents power that can be converted by water and light curtailment.

$$\min\ F_1 = \sum_{t}^{T}\sum_{i}^{n_{hy}} \eta_{hy}\left(S_{i,t} - Q_{i,t}^{H}\right) H_{i,t}\Delta t + \sum_{t}^{T}\sum_{j}^{n_{pv}}\left(P_{j,t}^{pv,\max} - P_{j,t}^{pv}\right) \quad (32)$$

2) NAVIGATION TARGET

Navigation requires a stable water level. In order to meet the navigation requirements, the virtual power plant aims to minimize the variance of the reservoir water level.

$$\min\ F_2 = \sum_{i}^{n_{hy}}\sum_{t}^{T}\left(Z_{i,t} - Z_i\right)^2 \quad (33)$$

Constraints include node power balance constraints, as shown in (34), and constraints of cascade hydropower, photovoltaic, and pumped storage units as shown in (1)-(20).

$$P_t^{Vpp} = \sum_{i}^{n_{hy}} P_{i,t}^{hy} + \sum_{j}^{n_{pv}} P_{j,t}^{pv} + \sum_{k}^{n_{pg}}\left(P_{k,t}^{pg} - P_{k,t}^{pp}\right) \quad (34)$$

IV. SOLUTION MATHODOLOGY

A. SOLUTION PROCEDURE

As for the congestion management problem involving VPP with cascade hydro-photovoltaic-pumped storage hybrid generators, solution procedure is illustrated in Figure 2. Firstly, VPP predicts the output of photovoltaic units and the electricity price in day-ahead market based on historical data, and offers day ahead scheduling plan. The day-ahead scheduling model of the VPP is given in (35)-(37).

$$F = \max\left\{\min\left(u(F_1), u(F_2)\right)\right\} \quad (35)$$

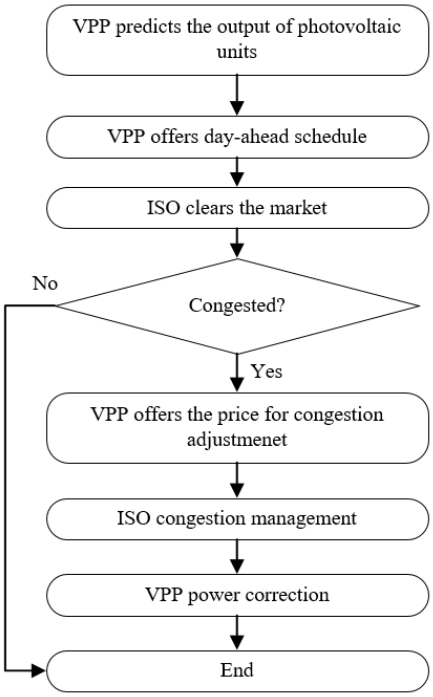

FIGURE 2. Procedure of congestion management involving VPP with cascade hydro-photovoltaic-pumped storage units.

$$u(F_i) = \begin{cases} 1 & f_i \le F_{i\min} \\ \left(\dfrac{F_{i\max} - F_i}{F_{i\max} - F_{i\min}}\right) & F_{i\min} < F_i < F_{i\max} \\ 0 & F_i \ge F_{i\max} \end{cases} \quad i = 1, 2 \quad (36)$$

$$s.t.\ (1) - (20)(37) \quad (37)$$

where (35) represents the objective function of day-ahead scheduling model of VPP. (36) is the normalization process of F_1 and F_2. When F_1 is regarded as the objective function of VPP day-ahead scheduling model, $F_{1\min}$ and $F_{2\max}$ can be derived from the optimization results. When F_2 is regarded as the objective function of VPP day-ahead scheduling model, $F_{1\max}$ and $F_{2\min}$ can be derived from the optimization results. As the paper focuses on congestion management, the day-ahead scheduling model of VPP is simplified. (35) and (36) convert the multi-objective model to single-objective model. Together with constraints (37), PSO algorithm is applied to solve the model and get the day-ahead output of VPP.

Then, the ISO clears the market seeking for its corresponding maximum social welfare. If the network is congested, a congestion management model considering the participation of VPP will be established to determine the power adjustment amount of VPP. Finally, VPP optimizes its internal resources and implements power correction.

B. SOLUTION APPROACH

The ISO congestion management model is a single-objective non-linear model that can be solved by Genetic Algorithm

(GA). The VPP power correction model is a multi-objective non-linear optimization model. This paper proposes a novel method called improved HNSGA-II to solve the Pareto fronts.

In this paper, an improved HNSGA-II algorithm is proposed to increase the mutation space and retain some infeasible solutions in the evolution process, which improves the population diversity, inhibits the occurrence of premature phenomenon to a certain extent and obtains better Pareto fronts.

1) HNSGA-II ALGORITHM

a: NON-UNIFORM MUTATION

Non-uniform mutation is the most common mutation operator used in the evolutionary algorithms. Assume $x = (v_1, v_2, \ldots, v_n)$ is one of the parent solutions.$v_k$is randomly selected from $[a_k, b_k]$for non-uniform mutation. The mutated solution is shown in (38).

$$x' = \left(v_1, \ldots, v_{k-1}, v'_k, v_{k+1}, \ldots, v_n\right) \tag{38}$$

where

$$v'_k = \begin{cases} v_k + \Delta\left(it, b_k - v_k\right), rnd = 0 \\ v_k + \Delta\left(it, v_k - a_k\right), rnd = 1 \end{cases} \tag{39}$$

$$\Delta\left(it, m\right) = m\left(1 - r^{\left(1 - \frac{it}{Imax}\right)^{\beta}}\right) \tag{40}$$

b: LOCAL SEARCH

Local search is applied to improve the accuracy of non-dominated solutions. Assume x and y are two non-dominated solutions, and x_s is the sub-generation solution. If x_s is superior to y, y should be replaced by the following method.

$$x_c = x_s + y \tag{41}$$

$$x_r = x_c + \delta\left(x_c - y\right) \tag{42}$$

In (42), the initial value of δ is 1.3. If x_r is superior to x_s, increase δ; otherwise, decrease δ. Repeat until x_r cannot be changed. If x_r is superior to x_s, y can be replaced by x_r; otherwise, y is replaced by x_s.

2) IMPROVED HNSGA-II ALGORITHM

In this paper, a novel method called improved HNSGA-II is developed by introducing Gauss mutation and constraint handling techniques.

a: GAUSS MUTATION

In evolutionary algorithms, mutation operators randomly perturb individuals at a certain mutation rate. Uniform mutation, non-uniform mutation, Gaussian mutation and Cauchy mutation are four common mutation operators. It is pointed out in [20] that the convergence effect of non-uniform mutation and Gauss mutation is better than that of Cauchy mutation and uniform mutation. In this paper, Gauss mutation is used instead of the original uniform mutation in NSGA-II to improve the convergence of the solutions. Besides, this paper adopts a mutation strategy combining random Gaussian mutation and dynamic Gaussian mutation. Random Gauss operator is applied in the early stage of searching process for large variation space. Dynamic Gauss operator is applied in the later stage of the searching process to accelerate the convergence speed and increase the accuracy of solutions.

Assume $x = (v_1, v_2, \ldots, v_n)$ as one of the parent solutions. v_k is randomly selected for Gauss mutation. The random Gauss operator is shown in (43).

$$v'_k = v_k + N\left(0, 1\right) \tag{43}$$

where $N\left(0, 1\right)$ means standard normal distribution.

The dynamic Gauss operator is given in (44).

$$v'_k = v_k + \left(1 - \frac{it}{Imax}\right) \times N\left(0, 1\right) \tag{44}$$

b: CONSTRAINT HANDLING TECHNIQUES

Feasible solutions dominate infeasible solutions in most of the constraint handling methods for multi-objective optimization problems. Therefore, some infeasible solutions near the edge of feasible region are discarded. This paper adopts the constraint handling method in [21] and keeps the infeasible solutions with small deviations from the constraints during the evolution process. These infeasible solutions are close to the edge of feasible region. The optimal solution can be approached simultaneously from the inside of the feasible region and the edge of the infeasible region, which improves the diversity of the optimal solution.

The multi-objective optimization problem can be simplified as:

$$\min f\left(x\right) = \left(f_1\left(x\right), \ldots, f_4\left(x\right)\right) \tag{45}$$

$$s.t.\ g_j\left(x\right) \le 0 \quad j = 1, 2, \ldots, q$$

$$h_j\left(x\right) = 0 \quad j = q+1, \ldots, p \tag{46}$$

The inequality constraints can be converted as:

$$\left|h_j\left(x\right)\right| - \varepsilon \le 0 \tag{47}$$

The constraints of solution x are modified and added to the objective function. The modified objective function is consist of distance value and penalty, which are given in (48).

$$f'_i\left(x\right) = d_i\left(x\right) + p_i\left(x\right) \tag{48}$$

The distance value can be calculated as:

$$d_i\left(x\right) = \begin{cases} C\left(x\right) & \alpha = 0 \\ \sqrt{\bar{f}_i\left(x\right) + C^2\left(x\right)} & \alpha \ne 0 \end{cases} \tag{49}$$

$$\bar{f}_i\left(x\right) = \frac{f_i\left(x\right) - f_i^{\min}}{f_i^{\max} - f_i\left(x\right)} \tag{50}$$

$$C\left(x\right) = \frac{1}{q}\sum_{j=1}^{q}\frac{c_j\left(x\right)}{c_j^{\max}} \tag{51}$$

$$c_j\left(x\right) = \begin{cases} \max\left(0, g_j\left(x\right)\right) & j = 1, \ldots, q \\ \max\left(0, \left|h_j\left(x\right)\right| - \varepsilon\right) & j = q+1, \ldots, p \end{cases} \tag{52}$$

$$c_j^{\max} = \max_x c_j\left(x\right) \tag{53}$$

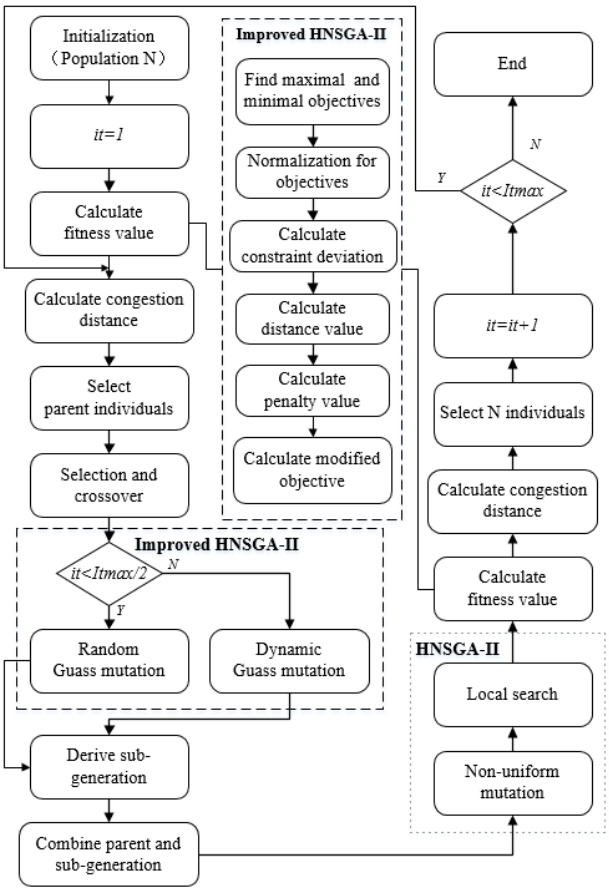

FIGURE 3. Improved HNSGA-II algorithm.

Equation (50) is the normalized function and (51) represents the constraint deviation. According to (49), if there is no feasible solution, $\alpha = 0$ and $d_i(x) = C(x)$. The distance value is determined only by the constraint deviation value. If there are feasible solutions, $\alpha \neq 0$. The distance value is determined by both objective function and constraint deviation.

The penalty value can be calculated as:

$$p_i(x) = (1-\alpha)\, C'(x) + \alpha \bar{f}_i(x) \tag{54}$$

$$C'(x) = \begin{cases} 0 & \alpha = 0 \\ C(x) & \alpha \neq 0 \end{cases} \tag{55}$$

It can be observed from the (54) that when there are more infeasible solutions, α is small and the penalty value is mainly determined by the first term on the right side of the formula. When there are few infeasible solutions, α is large and the penalty value is mainly determined by the second term on the right side of the formula. The population is more inclined to evolve towards solutions with better objective function values.

The algorithm flowchart is illustrated in Figure 3, where the improvement strategies are framed with dashed lines. In this paper, the combination of the maximum iteration number and crowding distance is adopted as the convergence criterion. Finally, the individuals with crowding distance of 1 in the population are selected as Pareto frontier. A common algorithm called maximum entropy method is applied to determine the best compromise solutions from the obtained Pareto solution set, which will not be specifically described in this paper.

TABLE 1. Congestion management prices for IEEE 30-bus system.

Units	1	2	3	4	5	6	VPP
Up ($/MW)	6	7.2	5.5	8	7.8	7.2	5.3
Down ($/MW)	2.1	1.6	1.9	1.9	1.7	2.3	1.5

TABLE 2. Parameters of units in the VPP.

Units	Efficiency	Capacity/MW
Hydropower 1	0.65	30
Hydropower 2	0.6	15
Pumped storage	0.95	15
Photovoltaic	0.9	25

V. ILLUSTRATIVE EXAMPLE

Based on simulation programs with Matlab on a PC with an 8GB RAM and a 2.6 GHz Intel Core i5-3320 M processor, this section takes IEEE 30-bus test system as an illustrative example to verify the efficiency of our proposed model.

The daily base load is 200MW and the price for load shedding is 200$/MWh. The adjustment prices are usually different from different units, which depends on the adjustment ability, willingness to participate in congestion management, policy factors and other parameters and performance of units. In this paper, for simplicity, we give the adjustment prices directly in Table 1. Hydropower units and pumped storage, which account for a large proportion of the VPP, have lower dispatch costs than thermal power units. So the power adjustment cost of VPP congestion management is supposed to be lower than that of conventional units. When the network is congested, VPP will have the priority to adjust its power output, which promotes the consumption of renewable energy.

VPP is connected to node 6, including 2 cascade hydropower stations, 1 photovoltaic power station and 1 pumped storage unit. Parameters of units in VPP is shown in Table 2. The basic parameters and navigation and ecological parameters of hydropower are given in Table 3 and Table 4. Load and actual irradiance curve are illustrated in Figure 4, where the rated irradiation is set to 1000W/m^2. The inflow histogram is depicted in Figure 5.

A. CONGESTION MANAGEMENT

Assume line 6-8 has fault and the network is congested. Congestion costs are listed in Table 5. Power adjustment after congestion management is depicted in Figure 6. It can be

TABLE 3. Basic hydropower parameters.

Hydropower	1	2
Initial level (m)	791	684
Normal storage level (m)	798	685
Backwater level (m)	790	680
Drain flow limit (m^3/s)	44	32

TABLE 4. Navigation and ecological parameters of hydropower.

Hydropower		1	2
Navigation	Climbing limit (m)	3	3
	Maximum variation (m)	5	5
Ecology	Ideal flow (m^3/s)	23	30
	Minimal satisfaction	15	22

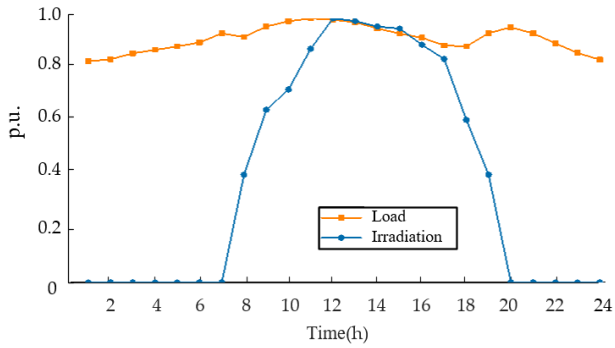

FIGURE 4. Load and actual irradiance curve.

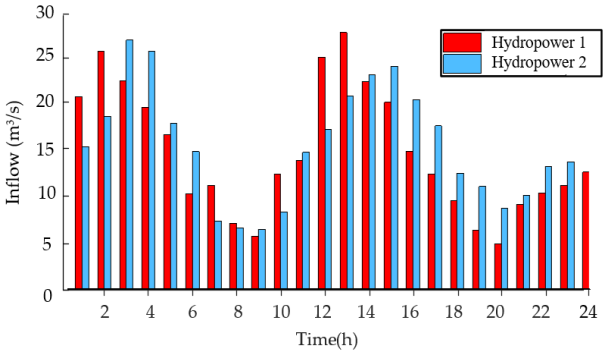

FIGURE 5. Inflow histogram.

observed that due to the lower upward adjustment price of VPP, the output of VPP increases. Meanwhile, the upward adjustments of unit 1, 3 and 6 decrease due to higher prices. The total congestion cost is reduced by 23.1%. Therefore, the participation of VPP in congestion management expands the power adjustment range of main grids and makes congestion management more economic.

B. VPP POWER CORRECTION

In this section, we analyze the power correction effect of VPP in the following 2 cases:

TABLE 5. Congestion costs ($).

Congestion costs	Without VPP	With VPP
1	1734	1359
2	516	450
3	1199	874
4	334	226
5	337	250
6	1364	770
VPP	0	289
Total	5484	4218

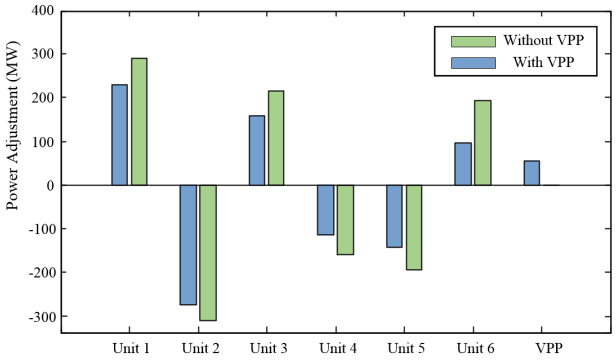

FIGURE 6. Power adjustment after congestion management for IEEE 30-bus system.

TABLE 6. Dispatch results of VPP in different cases for the illustrative example.

	Case 1	Case 2
Water and light curtailment F_1 (MWh)	0.5	83.1
Navigation conditions F_2 (m^2)	4.3	0.11
Ecological satisfaction F^{Eco}	38.3	37.6

Case 1: Minimal wind and light curtailment.

Case 2: Optimal navigation conditions.

Table 6 shows the dispatching results of VPP for case 1 and case 2. Outputs and water levels are illustrated in Figure 7 and 8, respectively.

It can be seen that the water and light curtailment in case 1 is smaller than that in case 2. In case 1, the outputs of hydropower 1 and hydropower 2 increase by 63.2MW and 6.9MW, respectively. The water storage of the pumped storage unit increases by 73.3MW. The output of hydropower 2 is larger before 13:00 and the output of hydropower 1 is larger after 13:00. Therefore, the water level in hydropower 1 gradually increases before 13:00 and then gradually decreases. The water level in hydropower 2 decreases before 13:00 and then increases.

In case 2, the navigation conditions are reduced by 97.2% and the ecological satisfaction is reduced by 0.7. Since case 2 takes the minimal variance of water level as the objective, the water levels of two hydropower stations are relatively

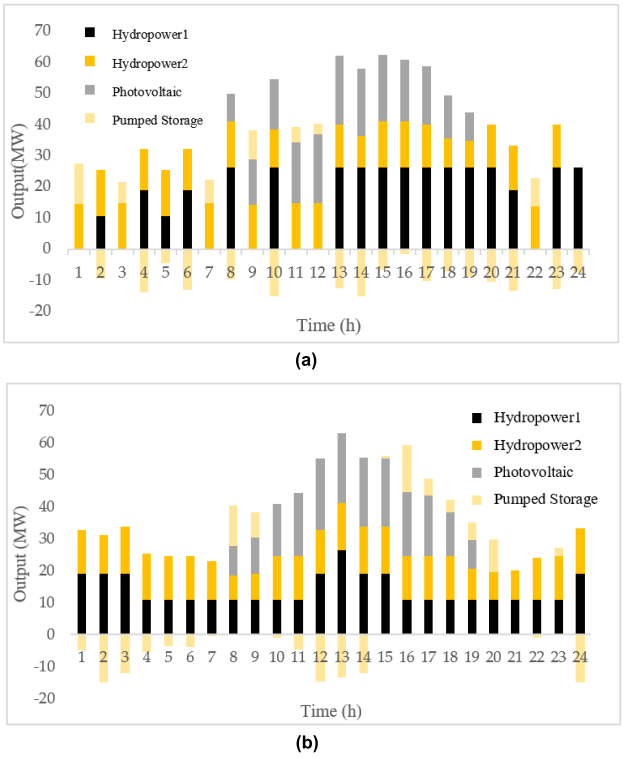

FIGURE 7. Outputs of units in VPP for different cases. (a) Case 1. (b) Case 2.

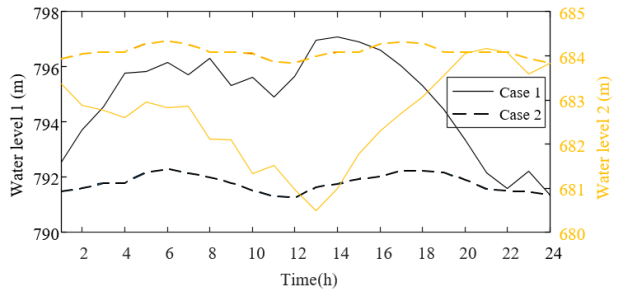

FIGURE 8. Water levels of cascade hydropower units in different cases.

stable. The daily water level differences in two cases are 1.03 meters and 0.49 meters, respectively.

C. ECOLOGICAL NEEDS

Figure 9 shows the objective values for different ecological conditions. In Figure 9(a), the objective is F_1. The water and light curtailment increases as $S_i^{\mathrm{E}\,\min}$ becomes larger. When $S_i^{\mathrm{E}\,\min}$ is small, the water level is stable and the navigation condition is 1.62. When $S_i^{\mathrm{E}\,\min}$ is in the range of 230000-230350m^3, the navigation condition changes greatly. In Figure 9(b), the objective is F_2. The water level variance increases as $S_i^{\mathrm{E}\,\min}$ becomes larger.

VI. CASE STUDY

In this section, we present numerical experiments on a modified IEEE 118-bus power system to demonstrate the performance of the proposed models and algorithms in large-scaled

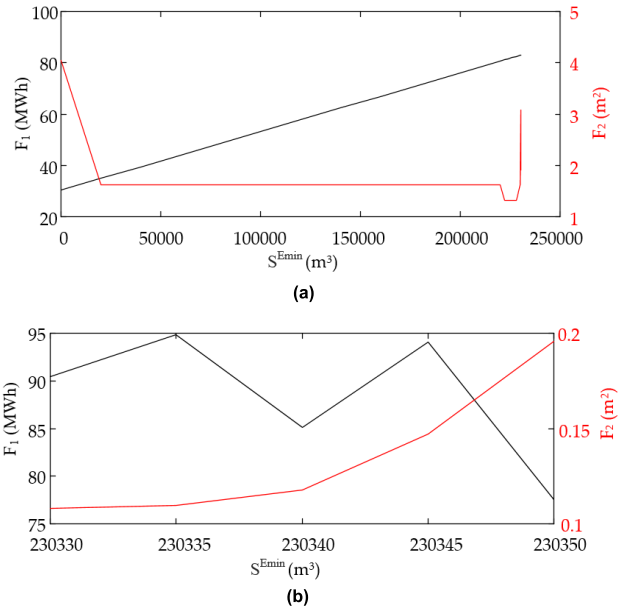

FIGURE 9. Objectives under different ecological conditions. (a) Minimal water and light curtailment. (b) Optimal navigation conditions.

TABLE 7. Congestion management prices for IEEE 118-bus system.

Unit: $/MW

Units	1	2	3	4	5	6	7	8	9
Up	7.8	9.4	7.2	10.4	10.1	9.4	7.9	8.8	6.6
Down	2.7	2.1	2.5	2.5	2.2	3.0	2.7	2.2	2.5
Units	**10**	**11**	**12**	**13**	**14**	**15**	**16**	**17**	**18**
Up	10.2	10.7	9.4	7.8	9.2	7.8	9.5	9.6	8.5
Down	2.6	2.2	3.2	2.5	2.1	2.7	2.5	2.3	3.2
Units	**19**	**20**	**21**	**22**	**23**	**24**	**25**	**26**	**27**
Up	8.0	10.3	7.2	11.2	9.2	8.7	7.3	10.2	7.6
Down	2.8	1.9	2.6	2.5	2.2	3.2	2.8	2.2	2.7
Units	**28**	**29**	**30**	**31**	**32**	**33**	**34**	**35**	**36**
Up	11.3	10.2	8.8	7.1	10.2	7.1	9.4	10.1	8.8
Down	2.5	2.1	3.1	3.0	2.3	2.6	2.3	2.0	2.9
Units	**37**	**38**	**39**	**40**	**41**	**42**	**43**	**44**	**45**
Up	7.3	8.8	7.7	9.6	10.0	9.8	8.4	9.0	7.6
Down	2.5	2.0	2.5	2.4	2.2	2.9	2.8	2.2	2.6
Units	**46**	**47**	**48**	**49**	**50**	**51**	**52**	**53**	**54**
Up	10.5	9.6	9.3	7.5	9.9	7.6	10.1	9.8	8.6
Down	2.4	2.0	3.2	2.7	2.0	2.6	2.6	2.3	3.3
Units	**VPP1**	**VPP2**	**VPP3**	**VPP4**	**VPP5**	**VPP6**	**VPP7**		
Up	6.1	5.7	6.4	6.1	6.3	5.9	6.4		
Down	2.1	2.1	2.3	2	2.5	2.2	2.2		
Units	**VPP8**	**VPP9**	**VPP10**	**VPP11**	**VPP12**	**VPP13**	**VPP14**		
Up	6.1	6.1	6.3	6.4	6.5	7.1	6.7		
Down	2.1	2.5	2.4	2.6	2.1	1.5	1.7		
Units	**VPP15**	**VPP16**	**VPP17**	**VPP18**	**VPP19**	**VPP20**			
Up	6.6	6.9	7.2	6.9	6.6	7.0			
Down	1.8	1.5	1.7	1.4	1.8	1.7			

systems. The simulation environment is identical to that of Section V.

The modified IEEE 118-bus power system depicted is consists of 54 thermal units, 186 branches and 99 loads. There are 20 VPPs connecting to node 2, 3, 7, 14, 16, 17, 20, 21, 22, 28, 73, 79, 83, 84, 96, 97, 109, 114, 117, 118. The congestion management prices for units and VPPs are shown in Table 7. Other parameters are identical to that to Section V.

TABLE 8. Dispatch results of VPPs in different cases for the case study.

	Case 1	Case 2
Water and light curtailment F_1 (MWh)	53.2	587.6
Navigation conditions F_2 (m²)	437.1	38.2
Ecological satisfaction F^{Eco}	748.3	672.1

TABLE 9. Comparison of algorithm performances.

	Convergence	Consistency	Extensity
NSGA-II	0.02	0.062	0.44
HNSGA-II	0.38	0.002	1
Improved HNSGA-II	0.60	0	0.83

A. SIMULATION RESULTS

Assume lines 8-28, 6-28, 10-21, 21-22, 15-23, 22-24, 24-25, 25-27 have fault and the network is congested. Power adjustments of 54 units after congestion management are depicted in Figure 10. VPP1-VPP12 participate in upward congestion management due to lower upward adjustment prices. VPP12-VPP20 participate in downward congestion management due to lower downward adjustment prices. It can be observed from Figure 10 that the upward and downward adjustments of all units decrease. Congestion management costs with and without VPPs are \$62350 and \$75182. The total cost is reduced by 17.1% due to the participation of VPP in congestion management.

Table 8 lists the dispatching results of VPPs for case 1 and case 2. The light and water curtailment in VPP is inversely proportional to the navigation conditions. Therefore, the water level will remain stable for optimal navigation conditions, resulting in more water curtailment. Furthermore, ecological needs is not a monotonic relationship with light and water curtailment and navigation conditions. It is necessary to take comprehensive consideration of three aspects, including ecological demand, light and water curtailment and navigation conditions, when dispatching units.

B. PERFORMANCE OF MULTI-OBJECTIVE ALGORITHMS

In this section, 3 indicators [19] are adopted to verify the performance of the proposed multi-objective algorithm.

1) CONVERGENCE

It represents the proportion of the solutions in real Pareto fronts, which is given in (56)-(58). E denotes the real Pareto front that combines the Pareto fronts of multiple algorithms by congestion degree. The greater the degree of convergence, the closer the solution to the optimal Pareto front.

$$C_k = \frac{n_{P^k} \bigcap E}{n_E} \tag{56}$$

$$P^k = \left\{ f_{k,i}^j \right\} \tag{57}$$

$$E = \bigcup_k P^k \tag{58}$$

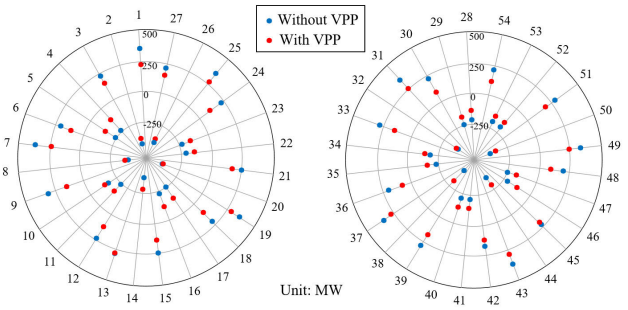

FIGURE 10. Power adjustments of 54 units after congestion management for IEEE 118-bus system.

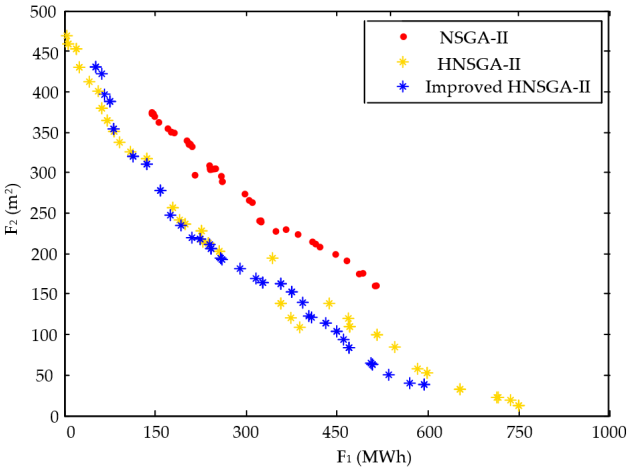

FIGURE 11. Pareto fronts in different algorithms.

2) CONSISTENCY

It denotes standard deviation of the distance between the solutions in Pareto solution set, which is obtained by (59)-(60). Smaller consistency indicates more uniform solution distribution.

$$d_{k,i} = \min_p \sqrt{\sum_j \left(f_{k,p}^j - f_{k,i}^j \right)^2} \tag{59}$$

$$S_k = \sqrt{\frac{1}{n_k} \sum_i \left(d_{k,i} - \overline{d_k} \right)^2} \tag{60}$$

3) EXTENSITY

It represents the average ratio of the solution space for a certain algorithm to the real solution space, which is calculated by (61). The greater the extensity, the closer the solution space to real Pareto front.

$$MS_k = \sqrt{\frac{1}{n} \sum_j \left\{ \frac{\min\left(f_k^{j,\max}, F^{j,\max} \right) - \max\left(f_k^{j,\min}, F^{j,\min} \right)}{F^{j,\max} - F^{j,\min}} \right\}^2} \tag{61}$$

The performance of different algorithms are shown in Table 9. Two-dimensional Pareto fronts in different

algorithms are depicted in Figure 11. Compared with NSGA-II, the local search technique in HNSGA-II improves the accuracy of non-dominated solutions, and the convergence and extensity are also improved. Gaussian mutation is applied in the improved HNSGA-II to increase the mutation space and the constraint handling technique guarantees the diversity of solutions. Therefore, the Pareto front is evenly distributed and the performance of convergence and consistency are the best of the three algorithms.

VII. CONCLUSION

In this paper, a two-stage optimization model is proposed to solve the congestion management problem involving VPP with cascade hydro-photovoltaic-pumped storage hybrid units. The proposed model also considers water and light curtailment, navigation, and ecological requirements. An improved HNSGA-II algorithm is presented to solve the multi-objective optimization problem. Simulation results show that the participation of VPP in congestion management can reduce the congestion costs of the system. The cascade hydro-photovoltaic-pumped storage combined dispatching can achieve multiple benefits in energy saving, navigation, and ecology. The performance of the proposed algorithm is significantly improved compared with NSGA-II and HNSGA-II.

REFERENCES

[1] R. Cao, J. J. Shen, C. T. Cheng, J. Zhu, and Y. Gao, "Multi-objective optimal control of cascaded reservoirs during drawdown period before flood season," *Proc. CSEE*, vol. 39, no. 10, pp. 2816–2827, Jun. 2019.
[2] J. T. Jia, "An optimal method of short-term scheduling for hydropower system with pumped-storage units," *Power Syst. Technol.*, vol. 41, no. 5, pp. 1597–1602, May 2017.
[3] W. Lyu, H. Wang, J. X. Yin, and X. Y. Zhu, "On ecological operation of cascade hydropower stations along Wujiang river in Guizhou province," *Adv. Water Sci.*, vol. 27, no. 6, pp. 918–927, Nov. 2016.
[4] J. T. Zhang, J. J. Shen, C. T. Cheng, and W. J. Niu, "Multi-objective optimal operation of cascade hydropower stations based on objective adjacent scale and marginal analysis principle," *Proc. CSEE*, vol. 39, no. 5, pp. 1268–1277, Mar. 2019.
[5] L. L. Sun, M. C. Zhao, N. Wang, Q. Q. Jia, and G. Y. Du, "Research of permitted capacity of distributed photovoltaic generation based on voltage deviation chance constrained," *Trans. China Electrotech. Soc.*, vol. 33, no. 7, pp. 1560–1569, Apr. 2018.
[6] L. Liu, J. F. Lin, and F. Y. Liu, "Analysis of maximum photovoltaic integrated capacity and its influences on distribution networks based on probabilistic load flow," *Electr. Eng.*, vol. 19, no. 7, pp. 15–20 and 26, Jul. 2018.
[7] H. J. Sun, J. H. Meng, and C. H. Peng, "Coordinated optimization scheduling of multi-region virtual power plant with wind-power/photovoltaic/hydropower/carbon-capture units," *Power Syst. Technol.*, vol. 43, no. 11, pp. 4040–4051, Nov. 2019.
[8] W. T. Hou and H. Wei, "A multi-source coordinated short-term dispatch model considering the dispatchability of nuclear power plants," *Trans. China Electrotech. Soc.*, vol. 33, no. 12, pp. 227–236, Jun. 2018.
[9] X. Tai, H. Sun, and Q. Guo, "Electricity transactions and congestion management based on blockchain in energy Internet," *Power Syst. Technol.*, vol. 40, pp. 3630–3638, Dec. 2016.
[10] Q. Sun, J. C. Peng, J. T. Pan, and P. Li, "Congestion management considering multi-time interval demand response," *Power Syst. Technol.*, vol. 34, no. 9, pp. 139–143, Sep. 2010.
[11] Q. S. Shi and S. D. Li, "Congestion management model and characteristics analysis with participation of interruptible load," *Proc. CSU-EPSA*, vol. 27, no. 7, pp. 48–53, Jul. 2015.
[12] Y. Q. Liu, W. U. Qiong, Z. Jiang, and A. I. Qian, "Management of transmission congestion of cross-region interconnected electricity market based on demand response," *Southern Power Syst. Technol.*, vol. 11, no. 2, pp. 78–86, Feb. 2017.
[13] B. F. Rad and M. Abedi, "Application of meta-heuristics algorithms in discrete model of steady-state load-shedding," in *Proc. 11th Int. Conf. Optim. Electr. Electron. Equip.*, Brasov, Romania, May 2008, pp. 173–177.
[14] E. Shayesteh, M. Parsa Moghaddam, S. Taherynejhad, and M. K. Sheikh-EL-Eslami, "Congestion management using demand response programs in power market," in *Proc. IEEE Power Energy Soc. Gen. Meeting Convers. Del. Electr. Energy 21st Century*, Pittsburgh, PA, USA, Jul. 2008, pp. 1–6.
[15] M. Esmaili, F. Ebadi, H. A. Shayanfar, and S. Jadid, "Congestion management in hybrid power markets using modified benders decomposition," *Appl. Energy*, vol. 102, pp. 1004–1012, Feb. 2013.
[16] M. Esmaili, N. Amjady, and H. A. Shayanfar, "Multi-objective congestion management by modified augmented e-constraint method," *Appl. Energy*, vol. 88, no. 3, pp. 755–766, Mar. 2011.
[17] S. Surender Reddy, "Multi-objective based congestion management using generation rescheduling and load shedding," *IEEE Trans. Power Syst.*, vol. 32, no. 2, pp. 852–863, Mar. 2017.
[18] S. A. Hosseini, N. Amjady, M. Shafie-khah, and J. P. S. Catalão, "A new multi-objective solution approach to solve transmission congestion management problem of energy markets," *Appl. Energy*, vol. 165, pp. 462–471, Mar. 2016.
[19] L. Chen, C. Yan, Y. Liao, F. Song, and Z. Jia, "A hybrid non-dominated sorting genetic algorithm and its application on multi-objective optimal design of nuclear power plant," *Ann. Nucl. Energy*, vol. 100, no. 2, pp. 150–159, Feb. 2017.
[20] S. H. Wen, J. H. Zheng, and M. Q. Li, "Comparison and research of mutation operators in multi-objective evolutionary algorithms," *Comput. Eng. Appl.*, vol. 45, no. 2, pp. 74–78, Jan. 2009.
[21] R.-H. Shang, L.-C. Jiao, C.-X. Hu, and J.-J. Ma, "Modified immune clonal constrained multi-objective optimization algorithm," *J. Softw.*, vol. 23, no. 7, pp. 1773–1786, Jul. 2012.

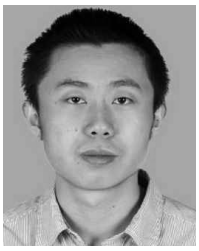

NAN LOU was born in 1989. He received the B.E. and M.E. degrees, in 2011 and 2014, respectively.

He is currently an Engineer with China Southern Power Grid Company Ltd. His research interests include power system dispatching operation and control, and power market operation.

YONG ZHANG was born in 1972. He received the B.E. and M.E. degrees, in 1994 and 1997, respectively.

He is currently a Senior Engineer with China Southern Power Grid Company Ltd. His research interests include power system dispatching operation and control.

YUQIN WANG was born in 1973. She received the B.E. and M.E. degrees, in 1995 and 1998, respectively.

She is currently a Senior Engineer with Dongfang Electronics Company Ltd. Her research interests include power system operation and dispatching, comprehensive energy, and power market operation.

QIXING LIU was born in 1985. He received the B.E. and M.E. degrees, in 2007 and 2010, respectively, and the Ph. D. degree in 2014.

He is currently an Engineer with China Southern Power Grid Company Ltd. His research interests include power market construction and operation, and power system dispatching operation and control.

HUIYONG LI was born in 1992. He received the B.E. and M.E. degrees, in 2014 and 2017, respectively.

He is currently an Engineer with China Southern Power Grid Company Ltd. His research interests include power system dispatching operation and control.

YU SUN was born in 1992. He received the B.E. and M.E. degrees, in 2014 and 2017, respectively.

He is currently an Engineer with Dongfang Electronics Company Ltd. His research interests include power system dispatching operation and control, and power market operation.

ZONGTIAN GUO was born in 1968. He received the B.E. degree in 1990.

He is currently a Senior Engineer with Dongfang Electronics Company Ltd. His research interests include power system dispatching operation and control, and power market operation.